Title: A measure of individual differences in the parametric sensitivity of the trigeminal blink reflex

Running head: Trigeminal blink sensitivity function

Author(s):
Eric A Kaiser[1†]; Edda B Haggery[1†], Dena P Garner[2], Vatinee Y Bunya[3], Geoffrey K Aguirre[1*]

[†]These authors contributed equally

[*]**Corresponding Author:**
Geoffrey K Aguirre
3400 Spruce Street, Philadelphia, PA 19104
aguirreg@upenn.edu

Affiliation Information for Authors:
[1]Department of Neurology, Perelman School of Medicine, University of Pennsylvania, Philadelphia, PA 19104
[2]Department of Health and Human Performance, The Citadel, Charleston, SC 29409
[3]Scheie Eye Institute, Perelman School of Medicine, University of Pennsylvania, Philadelphia, PA 19104

Key Words

- trigeminal system
- blink reflex
- individual differences

Abstract

The trigeminal blink response is an easily evoked brainstem reflex. Despite extensive investigation, there has been limited study of how parametric manipulation of the intensity of stimulation modulates the evoked response. The goal of this study was to measure the psychometric trigeminal reflex sensitivity function, test the resulting model parameters for differences between contralateral and ipsilateral reflex responses, and test for individual differences in sensitivity. We measured blink responses in 17 healthy, adult participants using airpuffs delivered to the cornea at five different, log-spaced intensities (3.5 - 60 PSI). Lid position over time was decomposed into amplitude, velocity, and shape components. We found that variation in blink amplitude was well fit with a two-parameter Weibull cumulative density function of log stimulus intensity. There was a reliable decrease in threshold sensitivity of the contralateral as compared to ipsilateral blink response. This decrease was consistent across participants despite substantial individual differences in the threshold and slope of the overall sensitivity function, suggesting that the laterality effect arises in the neural circuit subsequent to individual differences in sensitivity. We conclude that a parametric measure of trigeminal reflex sensitivity is a promising tool for examining neural mechanisms that modulate this response.

48 **Introduction**

49 The trigeminal blink reflex is an easily evoked, clinically relevant measure of brainstem
50 function. The cornea of the eye and periorbital skin are innervated by the ophthalmic (V1)
51 division of the trigeminal nerve. In the brainstem, the principal sensory nucleus of V receives
52 light-touch sensation from V1, while the nucleus caudalis receives both light touch and
53 nociceptive afferents.[1] Both of these nuclei project to local brainstem circuits that serve reflexive
54 functions, including eye blink.[2]

55 There is a long history of quantitative measurement of the human trigeminal blink reflex,
56 with a frequent approach being unilateral electrical stimulation of the supraorbital nerve or
57 cornea, and electromyographic (EMG) measurement of the binocular orbicularis oculi response.
58 Generally, the amplitude or latency of the response is measured for a fixed stimulus intensity, or
59 the threshold stimulus is found that evokes a criterion EMG response. There has, however,
60 been relatively little study of the effect of variation in somatosensory stimulus intensity upon the
61 evoked response. It is usually the case that there exists a range of log-spaced changes in
62 stimulus intensity that evoke linear changes in perception or physiologic response, following the
63 Weber-Fechner law. A focus upon measurement at response threshold can obscure individual
64 and population differences. For example, two groups may initiate a physiologic response at the
65 same threshold but differ in the amplification of that response with further increases in stimulus
66 intensity. Further, examination of the full sensitivity function, and how this function interacts with
67 other experimental variables, may be revealing as to the organization of the underlying neural
68 system.

69 Motivated by these observations, we develop here a quantitative measure of the blink
70 response evoked by parametric variation of a somatosensory stimulus. We used high-speed
71 infrared cameras to record lid position following puffs of air directed towards the cornea at log-
72 spaced pressure intensities. We measured how variation in stimulus intensity modulated
73 features of the blink response. We then tested the ability of these data to reveal reliable

differences in the sensitivity functions of the ipsilateral and contralateral blink response, individual differences in the sensitivity of the trigeminal system, and changes in blink responses across trials as a measure of habituation.

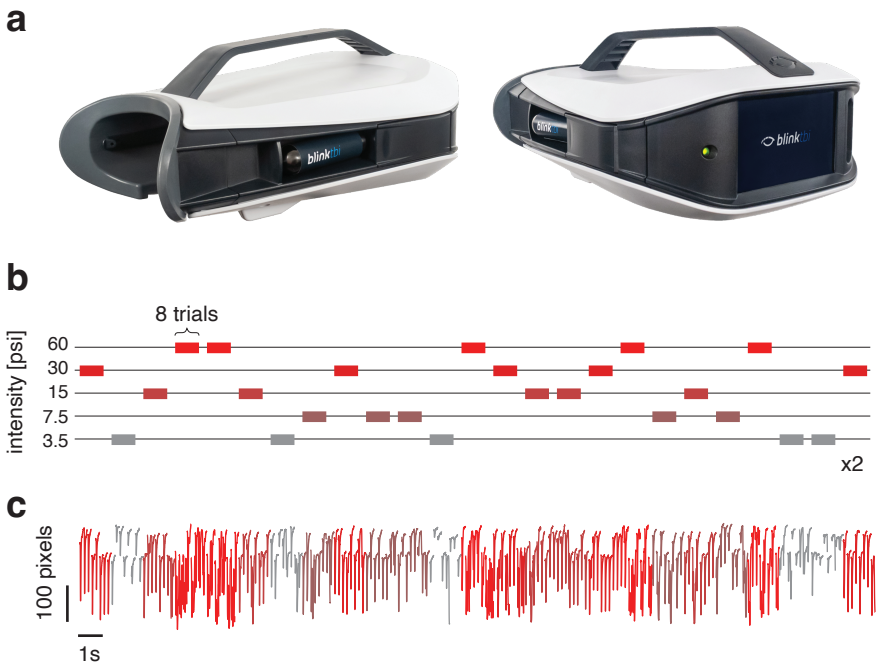

Figure 1. Experiment overview
(a) Blink responses were measured using an Eyestat Gen3 device, with custom modifications (not shown) to externalize pressure regulation. The participant placed their eyes within the mask assembly. **(b)** Counterbalanced pressure sequence. Each dash represents a single acquisition that presented a sequence of 8 airpuff trials. The air pressure used for the 8 trials was varied across acquisitions as shown. The entire sequence was administered twice. **(c)** Lid position over time obtained for Subject 14594. The data from each acquisition is color coded to indicate stimulus intensity, following the convention shown in panel b.

Results

Participants and data properties

We collected measurements from 17 participants who were recruited from a non-clinical setting and who denied a history of recurrent headache and acute or persistent symptoms from traumatic brain injury. Nine of the subjects were women, and the mean age of all participants was 25 (SD $\pm$ 4.03; range 20 to 32).

Each subject was studied using a custom-modified blink reflexometer (Figure 1a) that directed puffs of air at the cornea and lateral canthus. A total of 10 acquisitions of 8

airpuff trials was obtained at each of five, log-spaced pressure intensities with the order of acquisitions following a counter-balanced sequence (Figure 1b). IR video recordings of the eye ipsilateral and contralateral to the stimulus provided a measure of lid position over time (Figure 1c). From these recordings, the average blink response was obtained for each participant for each of the five stimulus intensities.

Our overall approach to the analysis of these data was to create a low-dimensional representation of the temporal components that constitute the blink response and then examine how the coefficients of these components changed with stimulus intensity.

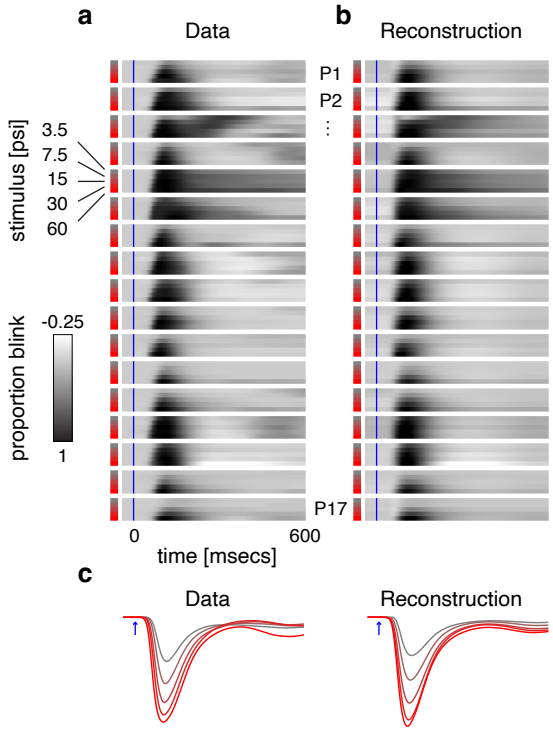

Figure 2. Observed and modeled blink responses
(a) The raster plot presents the temporal profile of lid position (averaged across acquisitions and ipsilateral and contralateral eyes) on each row, with blink depth indicated by grayscale shading. The responses to each of the five stimulus intensity levels are grouped together with each block running vertically corresponding to a different participant. The time of stimulus arrival at the cornea is indicated by a blue line. **(b)** The reconstruction of the data produced by the three temporal component model. There is good agreement between the reconstruction and the original data. **(c)** *(Left)* The average (across participant) blink response evoked by the five different stimulus intensity levels, with color indicating airpuff level from gray (3.5 PSI) to red (60 PSI). The blue arrow indicates the time of arrival of the airpuff to the cornea. *(Right).* The fit to these data provided by the 3 component temporal model.

Blink responses are well described by three temporal components

We first combined the responses from the eyelids ipsilateral and contralateral to the stimulus and examined the evoked blink response across participants and stimulus intensity levels. Figure 2a presents these data as a temporal raster plot with each evoked response in a row, and the grayscale level indicating the depth of lid movement. A similar general pattern was seen across subjects (grouped blocks) and stimulus intensity levels (increasing stimulus

intensity across rows within a block). Following the stimulus arrival at the cornea (vertical blue line), a blink of 100-200 msecs duration was initiated after a latency of 30-50 msecs. With increasing stimulus intensity, latency appeared to decrease, and blink duration and depth appeared to increase. Beyond these similarities, we also observed individual variation in the size and timing of the response and in the degree to which the response changed with stimulus intensity.

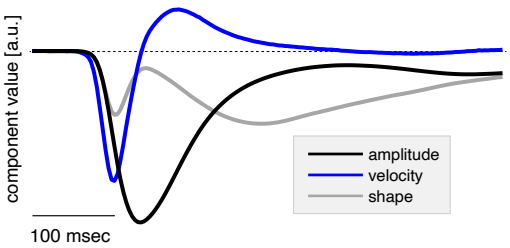

Figure 3. Temporal model components
Lid position vectors over time were fit using a three-component temporal model. These components corresponded to the amplitude of the blink (black), the first-derivative of amplitude and thus velocity (blue), and a third component that captured residual variation in shape (gray).

We created a low-dimensional temporal model of the blink response to describe this regularity and variation (Figure 3). The first component of the model (black) was simply the average lid position across all participants and stimulus levels and serves to capture the amplitude of the blink response. The second component (blue) was the first derivative of lid position and captured variation in the velocity and latency of the blink onset. The final “shape” component (gray) reflected variation in the overall shape of the evoked response, including individual differences in the tendency to hold the lid in a partially closed or more open state following the primary blink. Weighted combinations of these three components were used to fit a lid position vector, yielding three coefficients that summarized the response.

We fit the 85 average blink responses (17 participants x 5 stimulus levels) with the three-component temporal model. The reconstructed responses (Figure 2b) were a good match to the original data and accounted for 95% of the variance. The agreement between the data and the reconstruction can also be seen in the average (across subject) blink response at each stimulus pressure level (Figure 2c).

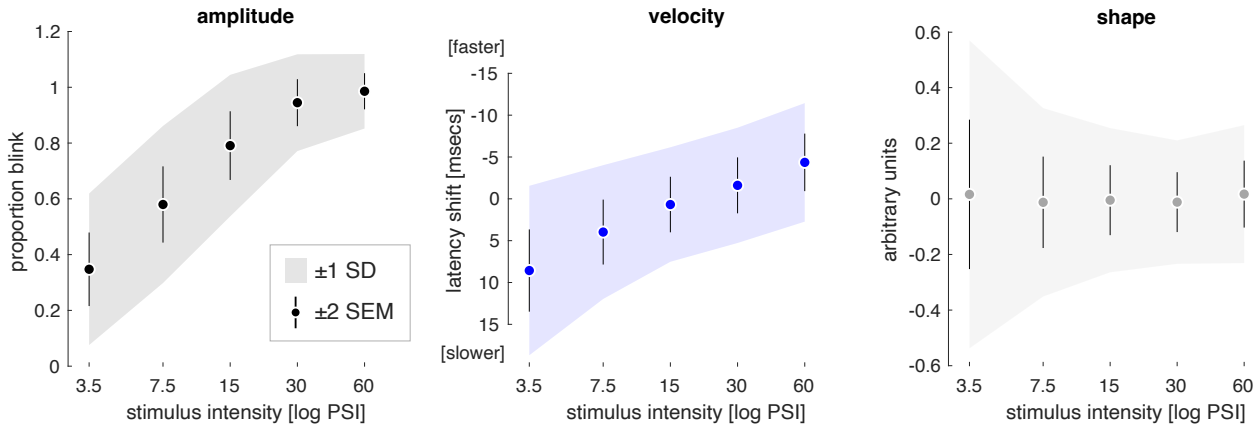

Figure 4. Coefficient values by stimulus intensity
Each plot presents the mean (across participants) coefficients for the three temporal components (amplitude, velocity, and shape) as a function of stimulus intensity (log PSI). The shaded area is ±1 standard deviation of the mean across participants, and the error bars ±2 standard errors.

Blink amplitude and velocity increase with stimulus intensity

We examined the value of the fit coefficients averaged across participants and sides (ipsilateral and contralateral) for each stimulus intensity level. This revealed a systematic effect of airpuff pressure upon blink response (Figure 4). Blink amplitude (expressed as the proportion of a complete blink) increased with stimulus intensity, with a roughly linear increase in blink depth related to log changes in stimulus pressure. Above 30 PSI, however, this function appeared to plateau. Blink velocity also increased with stimulus intensity: log changes in stimulus intensity led to roughly linear increases in blink velocity, reducing the latency of the response by about 15 msecs over the entire stimulus range. By contrast, no systematic relationship between stimulus intensity and the shape component was seen.

These findings confirm that aspects of the trigeminal blink response undergo parametric modulation with stimulus intensity. In subsequent analyses, we focus upon properties of the amplitude of the blink response, motivated by the reliability of the effect of stimulus intensity upon this measure, and the interpretability of the measure in terms of proportion of full lid closure.

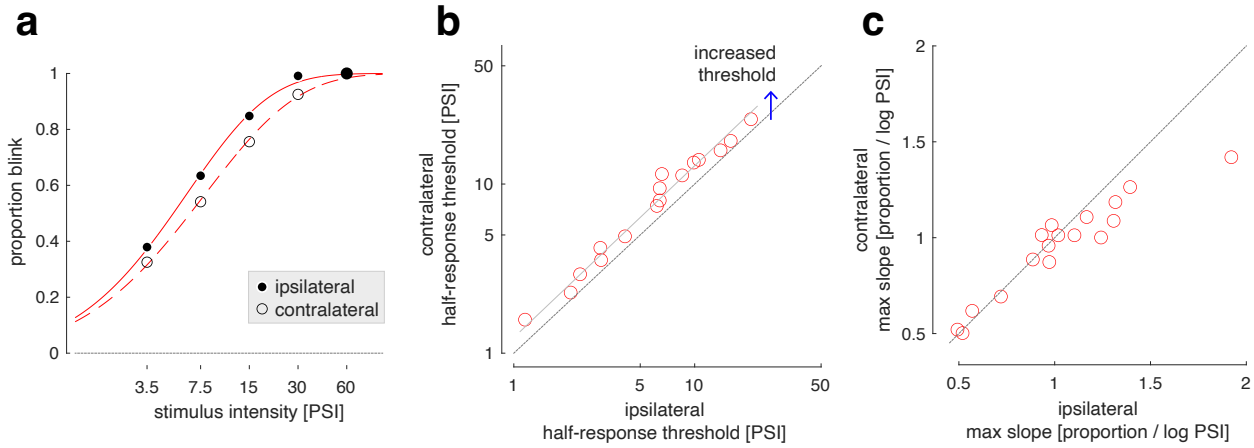

Figure 5. Ipsilateral versus contralateral blink responses.
(a) The mean (across participant) amplitude coefficients as a function of stimulus intensity, obtained separately for the eyelid ipsilateral (filled circles) and contralateral (open circles) to the stimulus. Amplitude is expressed as the proportion of a full eyelid closure. The points are fit with Weibull cumulative distribution function (red lines). **(b)** The psychometric function was fit to the amplitude data for each participant and side (ipsilateral and contralateral), yielding two parameters (half-response threshold and maximum slope). Here, each plot point indicates the half-response threshold parameters measured for a particular participant from the ipsilateral and contralateral eyelid. A linear fit to the set of points (gray line) is parallel to and shifted upwards from the unit slope (dashed line), corresponding to an ~0.1 log unit increased half-response threshold value measured from the contralateral as compared to the ipsilateral eyelid. **(c)** Each plot point indicates the maximum slope parameter value obtained from the ipsilateral and contralateral eyelid from each participant.

The contralateral blink response is subject to an increased stimulus threshold

The analyses up to this point combined the blink response measures from the eyelids ipsilateral and contralateral to the stimulus. We next tested if there are consistent differences in the sensitivity of the ipsilateral and contralateral response to trigeminal stimulation. We obtained the average amplitude coefficients across subjects for each stimulus level, separately for the ipsilateral and contralateral eye (Figure 5a). The measurements from each eye across pressure levels was then fit with a non-linear psychometric function (the Weibull cumulative distribution function). These fits provided a good account of the data and revealed that the intensity response function measured from the contralateral eye was shifted to the right as compared to the response from the ipsilateral eye. This property of the data indicates that generally higher intensity stimuli were required to evoke the same degree of lid closure in the contralateral eye as compared to the ipsilateral.

The Weibull function is under the control of two parameters that correspond to the stimulus intensity required to produce a 50% eye closure (the “half response threshold”), and the maximum slope of the change in eye closure with log changes in stimulus intensity. To assess the reliability of the difference in response between the ipsilateral and contralateral eye, we fit the amplitude coefficient data for the ipsilateral and contralateral eyelid separately for each participant. Figure 5b presents the half-response threshold values obtained for each participant from the ipsilateral and contralateral eyelid. While a wide range of values was seen, the plot points for all 17 participants were displaced ~0.1 log units above the unit slope line. A paired t-test across subjects of this measure between the contralateral and ipsilateral eye showed a significant difference ($t[16\ df] = 8.29$, $p = 3.499e\text{-}7$). This finding reveals that, across participants, there was a highly consistent, ~25% decrease in the threshold sensitivity of the response of the contralateral eyelid to trigeminal stimulation as compared to the ipsilateral eyelid.

Figure 5c presents the maximum slope of the psychometric function measured from the ipsilateral and contralateral eye for each subject. A wide range of values was again seen, although in this case the plot points did not systematically depart from the unit slope line, indicating a similar measurement from the two eyes. A paired t-test indicated that there was not a highly reliable difference in the slope value between the eyes ($t[16\ df] = 2.17$, $p=0.0453$).

We examined if the timing and shape of the blink response of the ipsilateral and contralateral eye differed. Across subjects and averaged across pressure levels, the velocity coefficient value was larger in the response from the contralateral eye as compared to the ipsilateral eye ($t[16\ df] = 3.83$, $p = 1.475e\text{-}03$), corresponding to an approximately 4 msec relative delay in the response of the contralateral eye. The blink response was also consistently narrower in time in the contralateral eye as compared to the ipsilateral eye, which was reflected in a difference in the shape coefficient ($t[16\ df] = 9.82$, $p = 3.528e\text{-}08$).

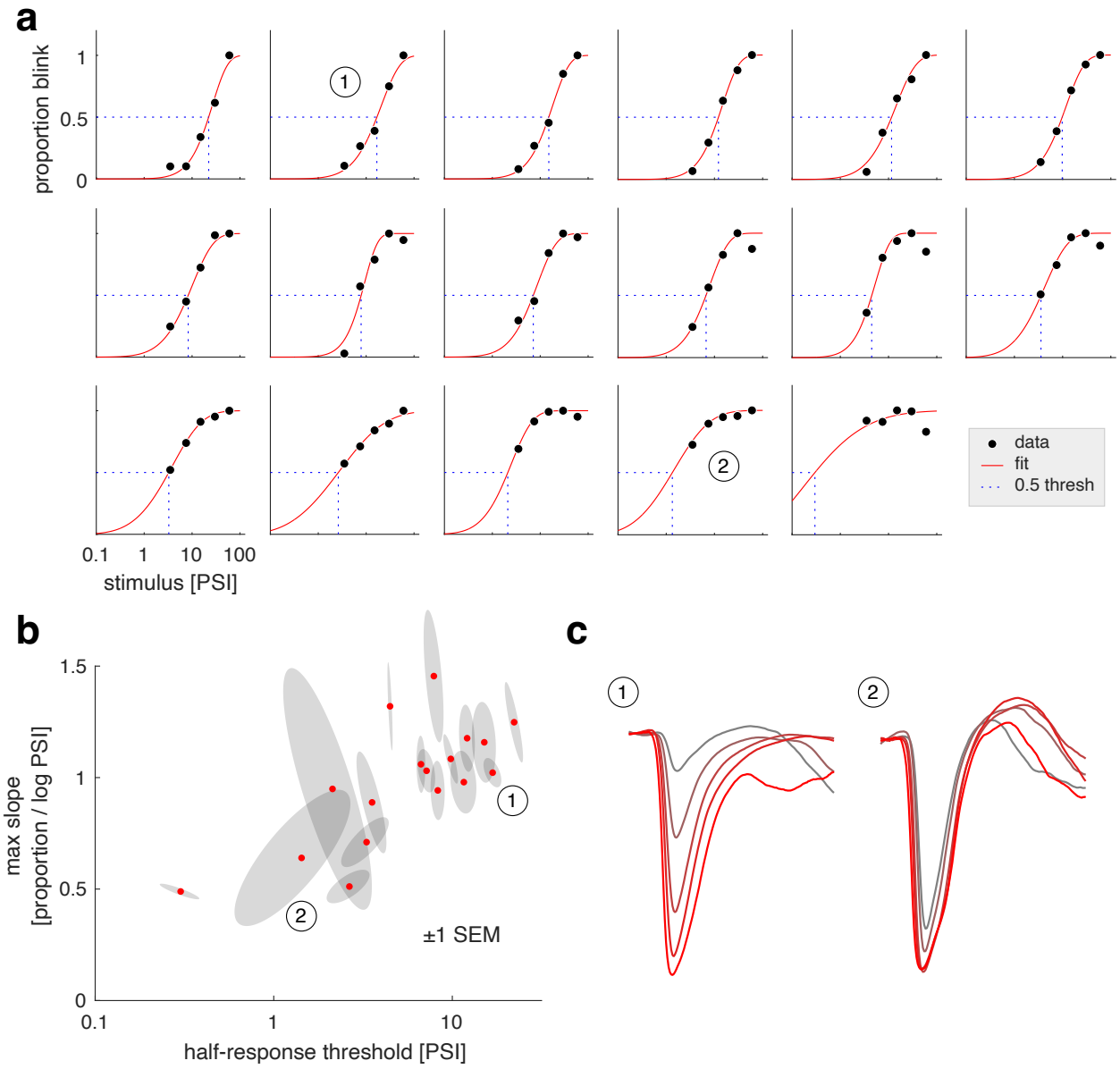

Figure 6. Individual differences in psychometric properties of blink amplitude. **(a)** Each sub-plot presents the amplitude coefficients for a participant as a function of stimulus intensity, averaged over acquisitions and the contralateral and ipsilateral eye. The fit of a Weibull cumulative distribution function is shown (red line), as is the half-response threshold value (dashed blue lines). Two example participants are identified with circled numbers, and these same participants are so indicated in subsequent panels. **(b)** The relationship between the half-response threshold and maximum slope parameters for each participant (red dots), surrounded by the bivariate normal distribution at one standard error of the mean obtained by bootstrap resampling across the 10 acquisitions (gray ellipses). **(c)** The average lid position plots at each stimulus intensity for two example participants (line color follows the convention of Figure 1).

Reliable individual differences in sensitivity parameters for blink amplitude

We next examined individual variation in the relationship between stimulus intensity and blink amplitude. Given that the difference between the ipsilateral and contralateral blink response was both small and consistent across individuals, we considered the blink responses averaged across the two eyelids. Figure 6a presents the fit of the Weibull function to the blink response amplitudes for each participant, ordered by the half-response threshold value obtained. For all participants, the psychometric function provided a good account of the effect of stimulus intensity upon blink amplitude. Across subjects, however, there was substantial variation in the form of the psychometric function. This variability can be seen both in the half-response threshold of the function (blue dotted lines), and in the maximum slope (steepness) of the fits.

The two parameters of the Weibull fit define for an individual the sensitivity of their blink response to varying trigeminal stimulation. Figure 6b plots the value of these two parameters for each participant, accompanied by the bivariate ellipse that indicates the standard error of the mean for the parameter estimates (obtained by bootstrap resampling across the 10 acquisitions at each stimulus level). Differences between individuals were substantially larger than the measurement uncertainty. There was a positive correlation between half-response threshold and maximum slope across participants ($r = 0.73$). The underlying differences in the blink response across stimulus levels is shown for two example participants in Figure 6c.

For roughly half of the participants, a decline in the amplitude of the blink was noted between the 30 and 60 PSI stimulus levels. Post-hoc examination of the data indicated that this phenomenon resulted from some subjects narrowing their palpebral fissure (i.e., squinting) during the set of eight trials with the highest stimulus intensity. This partial closing of the eye resulted in a smaller excursion of the lid in response to the stimulus.

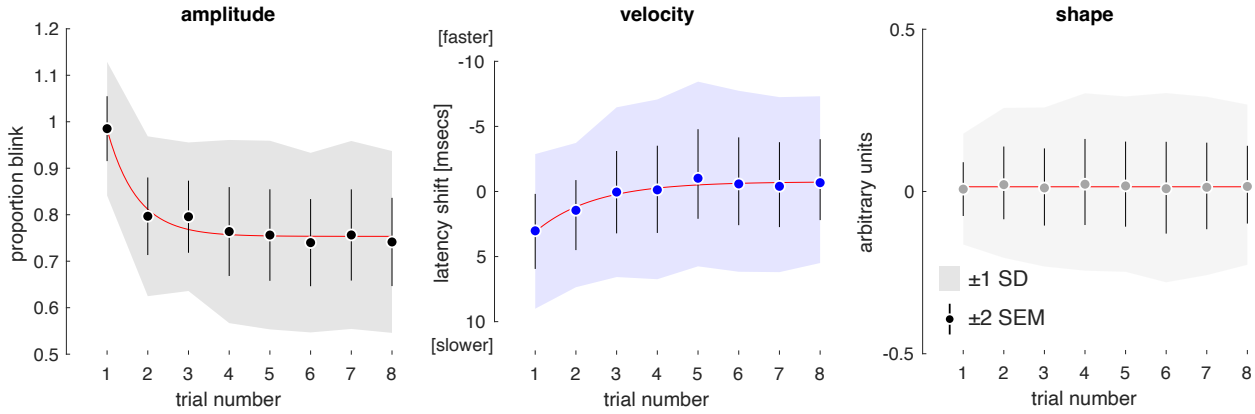

Figure 7. Coefficient values by trial number
Each plot presents the mean (across participant) coefficients for the three temporal components (amplitude, velocity, and shape) as a function of trial number. The shaded area is ±1 standard deviation of the mean across participants, and the error bars ±2 standard errors. The fit of an exponential function is shown (red line).

Changes in blink amplitude and velocity with repeated stimulation

Finally, we examined how the properties of the blink response changed over the 8 stimuli that were presented in rapid succession within each acquisition. For each participant, we fit the 3-component temporal response model to the average response across stimulus intensity, acquisitions, and sides, separately for each of the 8 trials. Figure 7 shows that across trial number, there was a decrease in the amplitude of the blink response, a slight increase in velocity, and no change in blink shape. These changes followed an exponential form, with the largest change in response coefficients being present between the first and second trial. We compared the R^2 of the exponential model fit in the data to the R^2 values obtained from fits to 10,000 permutations of the trial number order and found that the exponential form explains significant variance in the data for the amplitude (p=1.00e-4) and velocity (p=0.00110) components, but not shape (p=0.235)

Discussion

We have developed a measure of parametric variation in the trigeminal blink reflex and have shown that there are substantial individual differences in the sensitivity of this response to

245 changes in stimulus intensity. There is surprisingly little prior work that has measured how the
246 blink response varies with the intensity of a somatosensory stimulus. In a review of the clinical
247 assessment of the blink reflex, Esteban observed that increases in the electrical current used to
248 stimulate the supraorbital nerve evoked larger and earlier EMG components from the orbicularis
249 oculi (which mirrors our findings) but this informal observation was not quantified.[3] In perhaps
250 the closest precedent for the current study, Flaten and Blumenthal found that varying the
251 intensity of an airpuff between 1.5 and 4.5 PSI resulted in a monotonic increase in the amplitude
252 of the EMG voltage response from the orbicularis oculi.[4] There have been studies of parametric
253 variation in auditory[5] and visual stimulation,[6] which generally show an increase in amplitude and
254 a decrease in blink latency with increasing stimulus intensity. Overall, however, we are unaware
255 of prior work that has quantified how the form and timing of the blink changes with trigeminal
256 stimulus intensity, or how these changes covary within or across people.

257 EMG recording of the orbicularis oculi reveals temporally separated components of the blink
258 response. In primates, the early component (R1) is a small, ipsilateral reflex, while the later,
259 larger component (R2) is a bilateral response.[7] It is the R2 that that corresponds with the actual
260 blink of the eyelids[8] and is thus most related to our measurements. A third, still later component
261 (R3) has also been observed, particularly in response to noxious stimuli.[8]

262 We have shown that blink amplitude is well described by a two-parameter psychometric
263 function of the log of trigeminal stimulation intensity. The psychometric function is fully described
264 by the threshold and slope parameters. An intriguing but complicated topic concerns how
265 properties of neural circuits give rise to the particular values of these parameters that we
266 measure in behavior. While such an analysis is beyond the scope of the current study, we can
267 find the outlines of a mechanistic account in related areas of perceptual neuroscience. Studies
268 of decision-making have examined how the “readout” from populations of sensory neurons can
269 give rise to psychometric response functions of different forms.[9] At the output stage the varying
270 signals from a pool of sensory neurons are selected, weighted, and combined; different

271 mathematical operations that perform this readout are predicted to produce different
272 psychometric functions. Below, we draw from this theoretical work to help interpret the
273 variations in trigeminal sensitivity functions that we have measured.

274 We find a systematic difference between the threshold parameters measured from the
275 eyelid ipsilateral and contralateral to the stimulus. That is, a higher intensity stimulus is required
276 to evoke a given amount of lid movement in the contralateral eye as compared to the ipsilateral
277 eye, consistent with prior work.[10] A notable feature of our data is that, despite marked individual
278 variation in overall threshold and slope, the threshold difference between the ipsilateral and
279 contralateral blink response function is nearly identical across individuals (Figure 5b). This
280 suggests that the increased contralateral threshold arises from a common neural mechanism
281 across individuals, operating downstream from the source of individual variation. This is further
282 supported by our finding that the contralateral blink is consistently delayed by 4 milliseconds
283 compared to the ipsilateral response (in agreement with prior EMG measurements).[10] These
284 findings suggest that our measure of the trigeminal blink reflex are sensitive enough to detect
285 even small differences across a group of participants.

286 We find that there are substantial individual differences in the overall sensitivity of the
287 trigeminal blink reflex, as indexed both by half-response threshold and the slope of the response
288 function. There is a relatively strong correlation across individuals between these two
289 parameters, suggesting that people vary in a primary sensitivity axis that impacts both of these
290 parameters of the psychometric function. Given a set of neurons representing the stimulus, a
291 non-linear readout rule that amplifies the influence of the weakest responding neurons upon
292 motor output would be expected to flatten and shift the psychometric leftward, similar to the
293 effect of a max pooling rule in decision making [9]. We observe this kind of joint change in
294 parameters across our participants, with the most sensitive individuals demonstrating a large
295 blink response to even the smallest stimulus intensity, producing a low threshold and a shallow
296 slope parameter. The neural site of this variation could be present anywhere along the reflex

297 pathway. This variation is present in a relatively homogeneous population of young adults
298 without neurologic or ophthalmologic disease. An intriguing goal for future studies will be to
299 identify behavioral or perceptual correlates of this variation and the neural source of the
300 modulatory effect.

301 In other sensory domains, measurement of a stimulus-response function offers a
302 fundamental characterization of sensitivity that can have clinical importance. For example,
303 visual acuity measured over a range of stimulus contrast levels has been shown to better
304 separate patients from controls in multiple sclerosis and predict changes in retinal and brain
305 imaging measures.[11] For the blink reflex, it is possible that measurement of an entire response
306 function may more clearly reveal alterations in the sensitivity of the trigeminal system in clinical
307 disorders. An intriguing target is migraine, for which potentiation of pain signals from trigeminal
308 afferents is a cardinal feature. Despite the apparent association between the trigeminal system
309 and migraine, there is limited consensus regarding what (if any) alterations of somatic sensory
310 processing accompany headache disorders.[12] EMG measures of the trigeminal blink response
311 have been extensively studied in migraine, but with conflicting results regarding if an alteration
312 in response is present.[7] It may be the case that these studies, performed at a single stimulus
313 intensity level, have missed differences that would be revealed in the full trigeminal sensitivity
314 function.

315 Our measurement of the sensitivity of the blink reflex could be improved. First, the
316 delivery of the airpuff was accompanied by an audible hiss. As the auditory stimulus alone can
317 contribute to a blink response, future studies might have participants wear noise-cancelling
318 headphones to remove this component. Second, while the precise timing of each airpuff trial
319 could not be anticipated by the participant, it was the case that every trial presented a stimulus
320 of one non-zero intensity or another. Participants may blink in anticipation of a stimulus, and this

behavior might vary across individuals. The inclusion of acquisitions that present a 0 PSI airpuff would allow this behavior to be detected and modeled as part of the psychometric function.

In conclusion, application of a psychometric framework to the trigeminal blink reflex has allowed us to efficiently summarize the effects of laterality, participant, and repetition upon a complex temporal response. This analysis framework yields parameters that may, in future work, be related to the properties of neural circuits in quantitative models. Finally, measurement and modelling in people with migraine and other clinical disorders may be used to test for disruptions of trigeminal blink sensitivity, and to attribute these alterations to particular neural mechanisms.

Methods

Participants

We studied 17 participants recruited and tested by BlinkTBI Inc. These participants were recruited from The Citadel in Charleston, SC and from non-clinical settings in the surrounding Charleston community. Participants were at least 18 years of age, had no history of concussion within the past 5 years, and denied a history of recurrent headache. This study was approved by The Citadel Institutional Review Board, and all participants provided written consent.

The study was the subject of a pre-registration document (https://github.com/gkaguirrelab/preregistrations/tree/master/blink_2021). Our pre-registered enrollment goal was 15 subjects, and 17 were studied as the data from 2 subjects did not meet our original inclusion criteria. The analysis approach presented here departs substantially from our pre-registered plan, and allowed us to retain the measurements from all subjects. The supplementary materials present results that follow as closely as possible the pre-registered approach.

Operation of the device

347 Blink responses were measured using a custom-modified blink reflexometer (The
348 EyeStat device, Gen3, Blink TBI Inc) positioned over the eyes of the seated subject. During
349 each of many ~30 second acquisitions, the device directed 8 airpuffs from a pressurized CO_2
350 cartridge to the cornea and lateral canthus with the left or right eye selected randomly on each
351 of the 8 trials. The inter-stimulus-interval was jittered to reduce the ability of the participant to
352 anticipate the timing of the stimulus with at least 3 seconds between stimuli. The eyes were
353 illuminated with a ring of IR-LEDs that produced a corresponding ring of glint reflections on the
354 tear film. A pair of high-speed IR cameras (300 Hz, 800 x 600 pixels) were used to measure the
355 timing of obscuration of the glints by the movement of the eyelids. Recordings were made of the
356 movement of the eyelid ipsilateral and contralateral to the side on which the stimulus was
357 delivered. Microphones adjacent to the lateral canthus detected the airpuff, and the time of the
358 arrival of this pressure wave was used to sync recorded responses across trials.
359 During testing, subjects steadied themselves to receive the stimulus by holding the legs
360 of a tripod that supported the device. Room lights were left on during the session, although the
361 field of view of the subject was dark during data acquisition while their face was placed within
362 the device.
363 The device used in this study was custom modified by the manufacturer to externalize
364 pressure regulation. The CO_2 cartridge was connected by rigid tubing to an external pressure
365 regulator (Reg3000x, Leland Gas Technologies, South Plainfield, NJ), and then returned by
366 tubing to the EyeStat. Accuracy of specified air pressure levels was monitored with a National
367 Institute of Standards and Technology calibrated device (PressureMon2000, RegCo, Miami
368 Florida), which is certified to be accurate within ±0.2 pounds per square inch (PSI).

369 *Data collection*

370 The stimulus intensity was varied in separate acquisitions between five different, log-
371 spaced pressure values. A set of 26 acquisitions were obtained in each of two sessions, with

372 the order of pressure values following a pseudo-random, counterbalanced sequence de Bruijn
373 sequence [13]: [3, 3, 0, 2, 4, 4, 2, 0, 1, 3, 1, 1, 0, 4, 3, 2, 2, 3, 4, 1, 2, 1, 4, 0, 0, 3]; where 0 = 3.5
374 PSI, 1 = 7.5 PSI, 2 = 15 PSI, 3 = 30 PSI, and 4 = 60 PSI. To reduce the influence of non-
375 selective startle responses, data from the entire first acquisition were discarded, as was the first
376 trial of each acquisition. A total of 10 acquisitions were therefore obtained at each of the five
377 pressure levels, with each acquisition containing seven retained trials. The operator of the
378 device attempted to achieve the desired PSI value within ±1 PSI, and the actual, achieved
379 stimulus intensity was recorded for each acquisition. The unsigned mean deviation from nominal
380 values was 0.31 PSI, and in all cases did not exceed 1 PSI. For one participant, 3 of the 50
381 acquisitions included 4 trials instead of 8 due to operator error; we elected to retain the data
382 from this subject as this change in trial number was expected to have a negligible effect upon
383 the response measured for this subject.

384 There was a 30 - 60 second break following each acquisition. Each session was
385 approximately 50 minutes in duration, and the two sessions were separated by 1 to 5 days.

386 *Data pre-processing*

387 The raw data consisted of infrared videos of the eyelids during each trial. Initial
388 processing of these videos was conducted by Blink TBI Inc. using proprietary software. This first
389 stage of analysis provided a measure of lid position during each trial with 3.5 msec temporal
390 resolution, with all trials aligned to the time of arrival of the stimulus at the eye. All subsequent
391 analyses were performed using custom MATLAB software (Mathworks, Natick, Massachusetts).
392 The data and code needed to reproduce the analysis and figures presented here are publicly
393 available (https://github.com/gkaguirrelab/blinkCNSAnalysis).

394 The lid position over time was obtained for each subject for each stimulus intensity level,
395 averaging over all remaining trials and acquisitions. The raw measurement of lid position in units
396 of pixels was converted to a proportion of full eye closure by scaling all responses by the

397 maximum excursion observed for that subject and session. Full lid closure was observed for all
398 subjects at either the 30 or 60 PSI stimulus. This normalization accounted for variation in the
399 absolute size of the palpebral fissure across subjects and in the precise distance of the eye from
400 the infrared cameras.

401 The primary analyses of the study examined the set of 170 average lid position vectors
402 obtained from the 17 subjects at each of the 5 pressure levels, measured from the eye
403 ipsilateral and contralateral to the stimulus, averaged across trials and acquisitions.

404 *Three-component model of temporal response*

405 A model of the blink response over time was created to allow the temporal vector of lid
406 position to be summarized with a set of coefficients. The first component of the model was the
407 average profile of lid position over time, combined across subjects, pressure levels, and the
408 ipsilateral and contralateral eye. The second component was the first derivative of average lid
409 position. Next, a set of residual vectors was obtained by regressing each of the 170 vectors of
410 lid position upon these first two components. The set of residuals was then subjected to a
411 principal components analysis, and the first eigenvector was retained as the third component of
412 the model of temporal response. These three orthogonal components account for, respectively,
413 variation in the amplitude, velocity, and shape of the blink response.

414 A simple linear regression was then used to fit this three-component model to each lid-
415 position vector, yielding three coefficients. The effect of stimulus intensity upon the coefficients
416 was then examined, as well as the effect of other variables.

417 *Psychometric function relating blink amplitude and stimulus pressure*

418 A Weibull cumulative distribution function[14] was used to model the effect of log-
419 transformed stimulus pressure upon the coefficients that measured the amplitude of blink
420 response (expressed as the proportion of a full blink). Two parameters controlled the shape of
421 the fit, corresponding to the maximum slope of the function and the pressure at which 50% eye

closure was predicted. This function was fit to the amplitude coefficients obtained from each subject using the MATLAB *fmincon* function. A comparison of the fit parameters between the ipsilateral and contralateral eye was performed with a paired t-test across subjects.

A bootstrap resampling procedure was used to estimate the standard error of the mean of the parameters within subject. In this procedure, the set of 10 acquisitions obtained at each pressure level for a subject were randomly sampled with replacement, then the coefficients of the three-component model obtained for the synthesized average blink response, and then the parameters of the Weibull fit derived. The standard deviation of parameter values observed over 1,000 resampling iterations was taken as the standard error of the parameter mean.

Examination of habituation effects

For each subject, the blink response vectors for sequential trials within each acquisition were obtained and averaged over stimulus levels. After fitting with the three-component temporal model, the coefficients were examined for an effect of trial number.

References

1 May, P. J. & Porter, J. D. The distribution of primary afferent terminals from the eyelids of macaque monkeys. *Exp Brain Res* **123**, 368-381, doi:10.1007/s002210050582 (1998).

2 May, P. J. & Warren, S. Macaque monkey trigeminal blink reflex circuits targeting orbicularis oculi motoneurons. *J Comp Neurol* **529**, 2842-2864, doi:10.1002/cne.25130 (2021).

3 Esteban, A. A neurophysiological approach to brainstem reflexes. Blink reflex. *Neurophysiol Clin* **29**, 7-38, doi:10.1016/S0987-7053(99)80039-2 (1999).

4 Flaten, M. A. & Blumenthal, T. D. A parametric study of the separate contributions of the tactile and acoustic components of airpuffs to the blink reflex. *Biol Psychol* **48**, 227-234, doi:10.1016/s0301-0511(98)00018-0 (1998).

5 Peak, H. Intensity of stimulation and the amplitude and latency of the lid-reflex. *The American Journal of Psychology* **44**, 785-788 (1932).

6 Bixler, E. O., Bartlett, N. R. & Lansing, R. W. Latency of the blink reflex and stimulus intensity. *Percept Psychophys* **2**, 559-560, doi:https://doi.org/10.3758/BF03210267 (1967).

7 Vollono, C. in *Neurophysiology of the Migraine Brain Headache* (eds Gianluca Coppola & Wei-Ta Chen) Ch. 7, (Springer, 2021).

8 Rossi, B., Risaliti, R. & Rossi, A. The R3 component of the blink reflex in man: a reflex response induced by activation of high threshold cutaneous afferents. *Electroencephalogr Clin Neurophysiol* **73**, 334-340, doi:10.1016/0013-4694(89)90111-9 (1989).

9 Gold, J. I. & Ding, L. How mechanisms of perceptual decision-making affect the psychometric function. *Prog Neurobiol* **103**, 98-114, doi:10.1016/j.pneurobio.2012.05.008 (2013).

10 VanderWerf, F., Brassinga, P., Reits, D., Aramideh, M. & Ongerboer de Visser, B. Eyelid movements: behavioral studies of blinking in humans under different stimulus conditions. *J Neurophysiol* **89**, 2784-2796, doi:10.1152/jn.00557.2002 (2003).

11 Balcer, L. J. *et al.* New low-contrast vision charts: reliability and test characteristics in patients with multiple sclerosis. *Mult Scler* **6**, 163-171, doi:10.1177/135245850000600305 (2000).

12 Coppola, G. & Chen, W.-T. *Neurophysiology of the Migraine Brain*. (Springer, 2021).

13 Aguirre, G. K., Mattar, M. G. & Magis-Weinberg, L. de Bruijn cycles for neural decoding. *Neuroimage* **56**, 1293-1300, doi:10.1016/j.neuroimage.2011.02.005 (2011).

14 Wichmann, F. A. & Hill, N. J. The psychometric function: I. Fitting, sampling, and goodness of fit. *Percept Psychophys* **63**, 1293-1313, doi:10.3758/bf03194544 (2001).

Acknowledgements: none

Author Contributions: Conceptualization: E.K., V.Y.B., and G.K.A. Data curation: G.K.A. Formal analysis: E.B.H. and G.K.A. Funding acquisition: V.Y.B. and G.K.A. Investigation: E.B.H. and D.P.G. Methodology: E.B.H. and G.K.A. Project administration: E.B.H. Resources: D.P.G. Supervision: D.P.G. and G.K.A. Visualization: E.B.H. and G.K.A. Writing - original draft: E.K., E.B.H., and G.K.A. Writing - review & editing: E.K., E.B.H., D.P.G., V.Y.B., and G.K.A.

Data availability statement: The available raw data are of the form of lid position vectors recorded for every trial. These data, and the code needed to reproduce the analysis and figures presented here, are publicly available: https://github.com/gkaguirrelab/blinkCNSAnalysis

Additional Information:

Study Funding: R21 NS130565 (to GKA); P30 EY001583. In kind support provided by BlinkTBI Inc., including hardware, initial video processing, and engineering expertise.

Competing Interests: The authors declare no competing interests.

Figure Legends

Figure 1. Experiment overview
(a) Blink responses were measured using an Eyestat Gen3 device, with custom modifications (not shown) to externalize pressure regulation. The participant placed their eyes within the mask assembly. **(b)** Counterbalanced pressure sequence. Each dash represents a single acquisition that presented a sequence of 8 airpuff trials. The air pressure used for the 8 trials was varied across acquisitions as shown. The entire sequence was administered twice. **(c)** Lid position over time obtained for Subject 14594. The data from each acquisition is color coded to indicate stimulus intensity, following the convention shown in panel b.

Figure 2. Observed and modeled blink responses
(a) The raster plot presents the temporal profile of lid position (averaged across acquisitions and ipsilateral and contralateral eyes) on each row, with blink depth indicated by grayscale shading. The responses to each of the five stimulus intensity levels are grouped together with each block running vertically corresponding to a different participant. The time of stimulus arrival at the cornea is indicated by a blue line. **(b)** The reconstruction of the data produced by the three temporal component model. There is good agreement between the reconstruction and the original data. **(c)** *(Left)* The average (across participant) blink response evoked by the five different stimulus intensity levels, with color indicating airpuff level from gray (3.5 PSI) to red (60 PSI). The blue arrow indicates the time of arrival of the airpuff to the cornea. *(Right).* The fit to these data provided by the 3 component temporal model.

Figure 3. Temporal model components
Lid position vectors over time were fit using a three-component temporal model. These components corresponded to the amplitude of the blink (black), the first-derivative of amplitude and thus velocity (blue), and a third component that captured residual variation in shape (gray).

Figure 4. Coefficient values by stimulus intensity
Each plot presents the mean (across participants) coefficients for the three temporal components (amplitude, velocity, and shape) as a function of stimulus intensity (log PSI). The shaded area is ±1 standard deviation of the mean across participants, and the error bars ±2 standard errors.

Figure 5. Ipsilateral versus contralateral blink responses.
(a) The mean (across participant) amplitude coefficients as a function of stimulus intensity, obtained separately for the eyelid ipsilateral (filled circles) and contralateral (open circles) to the stimulus. Amplitude

is expressed as the proportion of a full eyelid closure. The points are fit with Weibull cumulative distribution function (red lines). **(b)** The psychometric function was fit to the amplitude data for each participant and side (ipsilateral and contralateral), yielding two parameters (half-response threshold and maximum slope). Here, each plot point indicates the half-response threshold parameters measured for a particular participant from the ipsilateral and contralateral eyelid. A linear fit to the set of points (gray line) is parallel to and shifted upwards from the unit slope (dashed line), corresponding to an ~0.1 log unit increased half-response threshold value measured from the contralateral as compared to the ipsilateral eyelid. **(c)** Each plot point indicates the maximum slope parameter value obtained from the ipsilateral and contralateral eyelid from each participant.

Figure 6. Individual differences in psychometric properties of blink amplitude.
(a) Each sub-plot presents the amplitude coefficients for a participant as a function of stimulus intensity, averaged over acquisitions and the contralateral and ipsilateral eye. The fit of a Weibull cumulative distribution function is shown (red line), as is the half-response threshold value (dashed blue lines). Two example participants are identified with circled numbers, and these same participants are so indicated in subsequent panels. **(b)** The relationship between the half-response threshold and maximum slope parameters for each participant (red dots), surrounded by the bivariate normal distribution at one standard error of the mean obtained by bootstrap resampling across the 10 acquisitions (gray ellipses). **(c)** The average lid position plots at each stimulus intensity for two example participants (line color follows the convention of Figure 1).

Figure 7. Coefficient values by trial number
Each plot presents the mean (across participant) coefficients for the three temporal components (amplitude, velocity, and shape) as a function of trial number. The shaded area is ±1 standard deviation of the mean across participants, and the error bars ±2 standard errors. The fit of an exponential function is shown (red line).

Title: A measure of individual differences in the parametric sensitivity of the trigeminal blink reflex

Running head: Psychometric Blink

Author(s):
Eric Kaiser[†]; Edda B Haggery[†], Dena P Garner, Vatinee Y Bunya, Geoffrey K Aguirre*

[†]These authors contributed equally

[*]**Corresponding Author:**
Geoffrey K Aguirre
3400 Spruce Street, Philadelphia, PA 19104
aguirreg@upenn.edu

SUPPLEMENTARY MATERIALS

The design of our study was the subject of a pre-registered protocol (https://github.com/gkaguirrelab/preregistrations/tree/master/blink_2021). Here, we present the results of the pre-registered analysis approach.

Methods

At the first stage of analysis, trials that contained a "valid" blink were identified, using a lid movement criterion defined within the BlinkCNS proprietary analysis software. The valid trials were retained, and a measure of nine blink "features" was derived from the recording made from the eye ipsilateral to the air puff stimulus. These features were:

- Area-under-the-curve (AUC) (msecs * pixels): Mean area-under-the-curve of the trajectory of the eyelid between the onset and completion of the blink as measured relative to the tonic position for that blink.
- Latency (msecs): Mean elapsed time between the application of the stimulus and the detection of the blink onset.
- Time under 20 (msecs): Mean elapsed time between the eyelid reaching a closed position and the eyelid moving more than 20 pixels back towards the tonic position.

- Time to open (msecs): Mean elapsed time between the eyelid reaching a closed position and the eyelid returning within threshold of the tonic position.
- Initial velocity (pixels / msecs): Mean average velocity over the first 7 frames of the blink.
- Time to close (msecs): Mean elapsed time between the detection of the onset of the blink and the eyelid reaching a closed position.
- Max closing velocity (pixels / msecs): Mean maximum velocity of the eyelid between the detected onset of the blink and the eyelid reaching the closed position.
- Max opening velocity (pixels / msecs): Mean maximum velocity of the eyelid between the eyelid reaching the closed position and the eyelid returning within threshold of the tonic position.
- Blink rate (count): Number of blinks performed by the eyelid between stimuli.

An acquisition was retained if it contained at least three valid blinks; the mean value for each feature from all valid trials within an acquisition was obtained. For each blink feature, we fit a linear model that related the log of the realized air pressure to the values of the blink feature, using the data from all acquisitions for the subject. A robust linear regression (the *fitlm* MATLAB function) was used to calculate the fit. The parameters of the fit were expressed as the slope of the relationship between log pressure and the blink feature, and as an offset value, which was the fitted value for the blink feature at 15 PSI.

The fit was performed first using the entire potential set of 50 acquisitions combined across the two testing sessions; for each subject we retained the R^2 of the model fit to the data for each feature. The sign of the slope of the model fit for each subject and blink feature was assigned to the R^2 value, supporting an examination of the mean, across subject, signed R^2 value as a test of the ability of the model to reliably account for experimental variance.

The reproducibility of these parameter values was examined by performing the linear model fit separately for the data from each of the two sessions, standardizing and grouping the resulting parameters across blink features, and then calculating the Pearson's r value between the session 1 data and session 2 data across participants.

Results

	Puff pressure model (R^2)	**Test-retest slope (r)**	**Test-retest slope (IQR)**	**Test-retest offset (r)**	**Test-retest offset (IQR)**
AUC	**0.81** [0.68, 0.92]	**0.78** [0.28, 0.99]	**33** [6, 116]	**0.64** [0.49, 0.99]	**16** [3, 278]
Latency	**0.98** [0.97, 0.98]	0.81 [-0.13, 0.98]	**24** [8, 51]	**0.92** [0.77, 0.99]	4 [0, 11]
Time under 20	**0.84** [0.76, 0.89]	-0.08 [-0.48, 0.96]	**57** [16, 1973]	0.17 [-0.14, 0.98]	**55** [12, 455]
Time to open	**0.79** [0.66, 0.90]	**0.82** [0.25, 0.99]	**59** [15, 133]	**0.61** [0.46, 0.99]	**38** [2, 231]
Initial velocity	**0.68** [0.53, 0.82]	**0.70** [0.09, 0.98]	**55** [10, 201]	**0.91** [0.77, 0.98]	**10** [4, 15]
Time to close	**0.43** [0.25, 0.61]	**0.79** [0.45, 0.99]	**131** [30, 249]	**0.73** [0.12, 0.97]	**8** [3, 16]
Close velocity	**0.72** [0.56, 0.85]	**0.89** [0.62, 1.0]	**31** [5, 137]	**0.90** [0.66, 0.98]	**11** [4, 20]
Open velocity	**0.58** [0.49, 0.69]	**0.86** [0.39, 0.99]	**35** [11, 107]	**0.75** [0.13, 0.96]	**14** [5, 37]
Blink rate	**0.58** [0.41. 0.74]	**0.56** [0.16, 9.91]	**132** [31, 633]	**0.85** [0.73, 0.96]	**34** [7, 51]

Table 1. Overview
Correlations and test-retest reliability by blink feature as a function of puff pressure. 95% CIs are described in brackets. Values for which the 95% CI excludes zero are bolded. *Column 1*: Pearson's R^2 for the blink feature as a function of log puff pressure combined across sessions. The value shown is the mean R^2 across subjects. *Column 2*: Mean test-retest reliability in the slope of the fit linear regression model for subjects between sessions 1 and 2. *Column 3:* Interquartile range for the slope agreement between sessions 1 and 2. *Column 4:* Mean test-retest reliability in the offset of the fit linear regression model for subjects between sessions 1 and 2. *Column 5:* Interquartile range for the offset agreement between sessions 1 and 2.